PERIODICA POLYTECHNICA SER. CHEM. ENG. VOL. 38, NOS. 1-2, PP. 47-56 (1994)

DETAILED MODELING OF UPFLOW ANAEROBIC FIXED FILM REACTORS

X. FLOTATS[1] and L. PUIGJANER[2]

[1] Environmental and Soil Sciences Dept.
Universitat de Lleida
Rovira Roure 177, 25006 Lleida, Spain

[2] Chemical Engineering Dept.
Universitat Politècnica de Catalunya, ETSEIB
Diagonal 647, 08028 Barcelona, Spain*

Received: July 20, 1994

Abstract

Upflow anaerobic fixed film reactors with high retention time or discontinuously loaded may result in rather large microbial aggregate fragments that are retained in the reactor. A structured model, based on the dynamics of a discrete bivariant distribution of sizes of bacterial aggregates and gas bubbles, has been developed which offers a methodological way to formulate hypothesis, detect some limit situations and achieve a mathematical synthesis of empirical knowledge about the considered phenomena. Experimental validation of the model has been carried out with satisfactory results.

Keywords: upflow anaerobic fixed film reactors.

1. Introduction

Anaerobic digestion processes are characterized by low available energy for bacterial growth and small growth rates, in comparison with other biological processes. That means the systems require some kind of biomass retention mechanisms, in order to achieve high reactor activity.

For anaerobic fixed film reactors, activity is considered to be due to microbial biofilm developed over the support matrix. This clearly requires the biofilm to be stationary and the net biomass grown fraction to be rapidly sloughed and washed-out, in order not to consider its activity. For low retention time fermentors, models based on biofilm kinetics allow to explain and simulate reactor performance with satisfactory results [1].

For upflow anaerobic fixed film reactors with high retention time or discontinuously loaded, biofilm sloughing or attrition may result in rather large microbial aggregate fragments that are retained in the reactor. Those microbial aggregate fragments that are retained in the reactor. Those aggregates consume substrate, grow, fragment into lower aggregate sizes, are

*Author whom correspondence should be addressed

transported downward by settling or upwards by attached or entrapped bubbles, and colonize new surfaces where a biofilm will be developed. Those systems are difficult to model and some empirical or semi-empirical 'black-box' models have been developed. Those models are useful to fit experimental data, but do not allow reactor performance explanation at all.

Biofilm and free microbial cell interaction have been studied by some researchers [2] and non-uniformity in free microbial aggregate sizes has been experimentally established for some types of bioreactors [3,4].

Aggregate size influences substrate uptake effectiveness, growth, settling velocity and reactor retention capacity. Although some experiences proved distribution size significance, few works have attempted to use population mass balance models [3, 5, 6].

In order to overcome the empirical model limitations, and to achieve an ordered framework capable of mathematical synthesis of empirical knowledge about involved phenomena, a structured model based on the dynamics of a discrete bivariant distribution of bacterial aggregates and gas bubbles diameters was developed.

2. Model Development

A particle will be defined as integrated by solid (bacterial aggregate) and gas (biogas bubble) phases. Aggregates and bubbles will be postulated to have spherical geometry. Biofilms will be postulated to have the same intrinsic properties as free aggregates, such as density, biomass concentration or substrate diffusivity, but attached to a vertically oriented support. Gas will be postulated to be produced in the aggregates and biofilms as spherical bubbles.

2.1. Particles Distribution Setting Up

Free aggregate diameters d belong to a total number of m size categories with class width w_a. Each diameter category is represented by d^i, equal to the median of that class. An aggregate of diameter d belongs to the category $(i, 0)$ if $d \in [d_i - \frac{w_a}{2}, d_i + \frac{w_a}{2})$, $d_i = (i - \frac{1}{2})w_a$, $i = 1, 2, ..., m$.

Free bubble diameters d belong to a total number of n size categories with class width w_b. Each diameter category is represented by its median d^j. A bubble of diameter d belongs to the category $(0, j)$ if $d \in [d^j - \frac{w_b}{2}, d^j + \frac{w_b}{2})$, $d^j = (j - \frac{1}{2})w_b$, $j = 1, 2, ..., n$.

A particle belongs to the category (i,j), $i = 0,1,..,m$, $j = 0,1,...,n$, if its biomass aggregate belongs to the $(i,0)$ category and its gas bubble belongs to the category $(0,j)$.

Particles concentration by volume, for each category, will be noted by C_i^j, $i = 0,1,...,m$, $j = 0,1,...,n$. The aggregate fraction for particles of (i,j) category is defined by $\mathbf{f}_i^j = \dfrac{(d_i)^3}{(d^j)^3 + (d_i)^3}$ and the bubble fraction by $(1 - \mathbf{f}_i^j)$.

For each category, settling or upward terminal velocity u_{oi}^j is calculated by fixing solid, gas and liquid phase densities, and using appropriate correlations for particles and bubbles.

2.2. Substrate Consumption

Substrate consumption rate for overall (i,j) category particles will be noted λ_i^j and the rate for the biofilm will be noted λ_x. The Monod type kinetics, $\mu_M = \dfrac{\widehat{\mu} C_B}{K_s + C_B}$, and constancy of Y, the biomass yield on the substrate, D_x, the effective diffusivity of the substrate in an aggregate and X_o, the biomass concentration in an aggregate, will be postulated.

The substrate consumption rate per unit of aggregate volume varies with the aggregate size, the bulk-liquid substrate concentration C_B and the relative aggregate/fluid velocity due to internal and external substrate transport resistances. This variation is characterized by the effectiveness factor η, η_i^j for (i,j) category particles and η_x for biofilm. This factor will be calculated by numerical approximation of the diffusion/reaction equation for a given aggregate geometry, including external transport limitations as a boundary condition [8].

2.3. Growth

The growth of particles is due to the growth of aggregate fraction, due to synthesized biomass from substrate consumption, and the growth of bubble fraction, due to the gaseous metabolites produced.

For the (i,j) category, growth is represented as an increase in the concentration C_i^j due to the transition of particles from the $(i-1, j-l)$ category, and a decrease due to the transition of (i,j) particles to the category $(i+1, j+k)$ of bigger sizes.

Substrate consumption by biofilm implies, as for spherical aggregates, a growth of biofilm volume V_x. Biofilm gas production is postulated to increase free bubbles concentration of the $(0,1)$ category.

2.4. Particle Fragmentation

Production of gaseous metabolites in the aggregates may reduce microbial cell cohesion and leads to particle disintegration. EDELSTEIN and HADAR [5] define fragmentation rate as a function of fluid shear stress and BEEFTINK and VAN DEN HEUVEL [6] propose that this rate is a function of substrate consumption rate and biomass concentration in the aggregates, which decreases with bacterial decay. In order to simplify expressions no decay rates will be considered and it will be postulated that fragmentation rate for a given category (p,j) is proportional to substrate consumption rate λ_i^j and particle gaseous fraction $(1 - \mathbf{f}_p^j)$, with f_{fr} as a constant proportionality factor.

The fragmentation process for a given (p,j) category is represented by a decrease in its concentration, an increase in the $(0,j)$ free bubbles category and an increase in free aggregates of lower size categories. As in BEEFTINK and VAN DEN HEUVEL model [6], it will be postulated that an 'A' fraction of a disintegrated aggregate is split into two halves, while the remaining part $(1 - a)$ is incorporated in the smallest type of free aggregate $(1,0)$.

2.5. Particle Axial Collisions with Support

There are experimental evidences that upward particle axial collisions with support enhace phase separation and aggregates confination. It will be postulated that all collisions lead to phase separation. The collision probability P_x, per unit of length, will be calculated as the ratio between the support section and the free flow section $\overline{S}_x$, if there are distribution support changes at the given height of the reactor.

Axial collision for (i,j) particles is represented by a concentration decrease in this category and an increase in $(i,0)$ and $(0,j)$ categories.

2.6. Bacterial Attachment

Biofilm development on a surface exposed to a fluid flow is the net result of several processes: Transport of microbial cells to surface, microorganisms attachment, growth on the surface and partial detachment caused by fluid shear stress [2].

The rate of increase in the biofilm volume V_x at a given reactor height, by attachment of microbial cells assumed to belong to the $(1,0)$ category, is postulated to be the product of the particles flux φ_1^0, its probability to contact biofilm surface P_T and the sticking efficiency P_f, estimated as a function of shear stress [7].

2.7. Biofilm Detachment

Once the biofilm thickness δ_x exceeds the laminar sublayer thickness δ, shear stress increases dramatically and so does biofilm removal rate [7]. Although studies have shown that removal, by attrition or sloughing, is a continuous process during biofilm development [2], in order to simplify expressions it will be postulated that there is a detachment when $\delta < \delta_x$. The biofilm fraction placed out of δ bound will be removed and incorporated into suspended biomass as $(1,0)$ category particles.

2.8. Vertical Transport of Particles

Vertical transport of particles will be modelled by evolution equations of a suspension composed by inert particles of various diameters and densities, using Richardson–Zaki equation and taking into account that the velocity for each category is controlled by the overall particle concentration at a given height of the reactor.

2.9 Setting-up the Model

Evolution equations for the particle concentration C_i^j and the bulk-liquid substrate concentration C_B in a differential volume of height dx and section $\overline{S}_x$, and the evolution equation for the biofilm volume V_x of height dx and section S_x, at a given height x in a L height reactor, with the rates as defined in *Table 1*, are

Table 1
Rates involved in model definition

	Particles	Biofilm
Growth	$(\Gamma_{gr})_i^j = \mu_M (d_i)^3 \left(\eta_{i-1}^{j-l} \frac{C_{i-1}^{j-l}}{(d_i)^3 - (d_{i-1})^3} \frac{\mathbf{f}_{i-1}^{j-l}}{\mathbf{f}_i^j} - \eta_i^j \frac{C_i^j}{(d_{i+1})^3 - (d_i)^3} \right),$	$\Gamma_{gr} = \eta_x V_x \mu_M$
	$i = 1, 2, ..., m-1; \quad j = 0, 1, ..., n$	
Fragmentation	$\left(\Gamma_{fr}\right)_p^j = -f_{fr} \lambda_p^j (1 - \mathbf{f}_p^j) C_p^j,$	
	$p = 1, 2, ..., m; \quad j = 1, 2, ..., n$	
	$\left(\Gamma_{fr}\right)_i^0 = a \sum_{j=1}^{n} \sum_{p=c}^{d} \mathbf{f}_p^j \left(\Gamma_{fr}\right)_p^j, \quad i = 1, 2, ..., m$	
	$\left(\Gamma_{fr}\right)_1^0 = (1-a) \sum_{j=1}^{n} \sum_{p=1}^{m} \mathbf{f}_p^j \left(\Gamma_{fr}\right)_p^j$	
	$\left(\Gamma_{fr}\right)_0^j = \sum_{p=1}^{m} (1 - \mathbf{f}_p^j) \left(\Gamma_{fr}\right)_p^j, \quad j = 1, 2, ..., n$	
Attachment	$(\Gamma_{at})_i^j = -\frac{1}{\overline{V}_x} \Gamma_{at}, \quad i = 1; \quad j = 0$	$\Gamma_{at} = \varphi_1^0 \overline{S}_x P_T P_f$
	$(\Gamma_{at})_i^j = 0, \quad i = 0, 2, 3, ..., m; \quad j = 0, 1, ..., n$	
Detachment	$(\Gamma_{dt})_i^j = -\frac{1}{\overline{V}_x} \Gamma_{dt}, \quad i = 1; \quad j = 0$	$\Gamma_{dt} = -\frac{(S_x(\delta_x) - S_x(\delta)) u_1^0 \overline{S}_x(\delta_x) \varepsilon_p}{\overline{S}_x(\delta) - \overline{S}_x(\delta_x)(1 - \varepsilon_p)}, \quad \delta < \delta_x$
	$(\Gamma_{dt})_i^j = 0, \quad i = 0, 2, 3, ..., m; \quad j = 0, 1, ..., n$	$\Gamma_{dt} = 0, \quad \delta \geq \delta_x$

Table 1
Rates involved in model definition (continued)

	Particles	Biofilm
Axial collision with support	$(\Gamma_{ac})_i^j = P_x u_i^j C_i^j, \quad u_i^j < 0,$ $(\Gamma_{ac})_i^j = 0, \quad u_i^j \geq 0,$ $i = 1, 2, ..., m; \quad j = 1, 2, ..., n$ $(\Gamma_{ac})_i^0 = \sum_{j=1}^{n} \mathbf{f}_i^j (\Gamma_{ac})_i^j, \quad i = 1, 2, ..., m$ $(\Gamma_{ac})_0^j = \sum_{i=1}^{m} (1 - \mathbf{f}_i^j)(\Gamma_{ac})_i^j, \quad j = 1, 2, ..., n$	
Biofilm gas production	$\left(\Gamma_{bg}\right)_i^j = B_g \frac{\lambda_x}{\overline{V}_x}, \quad i = 0; \quad j = 1$ $\left(\Gamma_{bg}\right)_i^j = 0, \quad i = 0, 2, 3, ..., m; \quad j = 0, 1, ..., n$	
Substrate consumption	$\lambda_i^j = \eta_i^j \mu_M \overline{V}_x \frac{X_0}{Y} \mathbf{f}_i^j C_i^j,$ $i = 1, 2, ..., m; \quad j = 0, 1, ..., n$	$\lambda_x = \eta_x V_x \frac{X_0}{Y} \mu_M$
Vertical transport	$(\Gamma_{tr})_i^j = \frac{\partial \varphi_i^j}{\partial x}, \quad \varphi_i^j = u_i^j C_i^j, \quad \varepsilon_p = 1 - \sum_{j=0}^{n} \sum_{i=0}^{m} C_i^j,$ $u_i^j = u_{oi}^j \varepsilon_p^{n_i^j - 1} - \sum_{k=0}^{m} \sum_{l=0}^{n} u_{ok}^l \varepsilon_p^{n_k^l - 1} C_k^l + \frac{Q(t)}{\overline{S}_x}$	

$$\frac{\partial C_i^j}{\partial t} = (\Gamma_{tr})_i^j + (\Gamma_{gr})_i^j + (\Gamma_{fr})_i^j + (\Gamma_{at})_i^j + (\Gamma_{dt})_i^j + (\Gamma_{ac})_i^j + (\Gamma_{bg})_i^j,$$

$$\frac{\partial V_x}{\partial t} = \Gamma_{gr} + \Gamma_{at} + \Gamma_{dt},$$

$$\frac{\partial C_B}{\partial t} = \frac{\partial v C_B}{\partial x} - (\sum_{i=1}^{m}\sum_{j=0}^{n} \lambda_i^j + \lambda_x)/\overline{V}_x \varepsilon_p,$$

$$i = 0, 1, ...m, \quad j = 0, 1, ...n, \quad (i, j) \neq (0, 0), \quad x \in [0, L],$$

with the appropriate boundary and initial conditions for a given reactor configuration [8].

3. Results and Discussion

Thirty days process numerical simulations have been obtained, using a 7×7 particles bivariant distribution and the parameter values and initial conditions showed at *Table 2.*

Table 2
Parameter values and initial conditions used for numerical simulations

$C_{Bin} =$	7.0 kg QOD·m^{-3}	$D_\ell =$	$0.5 \cdot 10^{-7}$ m^2·s^{-1}
$Q(t) =$	$0.0794 \cdot \Theta^{-1}$ m^3·day^{-1}	$D_s =$	$0.75 \cdot 10^{-8}$ m^2·s^{-1}
$\Theta =$	0.2, 1.0, 1.8, ..., 9.8 days	$\nu_\ell =$	$7.73 \cdot 10^{-7}$ m^2·s^{-1}
$d_m =$	$0.3 \cdot 10^{-3}$ m	$\rho_g =$	1.15 kg·m^{-3}
$d^n =$	$1.0 \cdot 10^{-3}$ m	$\rho_\ell =$	1000 kg·m^{-3}
$m =$	7	$\rho_s =$	1030 kg·m^{-3}
$n =$	7	$B_g =$	0.75 m^3 gas·(kg QOD)$^{-1}$
$X_0 =$	150 kg biomass·m^{-3}	$f_{f_r} =$	0.7 (kg QOD)$^{-1}$
$Y =$	0.12 kg biomass·(kg QOD)$^{-1}$	$a =$	0.6
$\hat{\mu} =$	0.25 day^{-1}	$P_x =$	0.19
$K_s =$	120 kg QOD·m^{-3}	$L =$	2 m
Initial conditions ($x \in [0, L]$):			
$C_i^j(x,0) =$	$2.0 \cdot 10^{-3}$, $i = 1, j = 0$	$S_x(x,0) =$	$1 \cdot 10^{-4}$ m^2
$C_i^j(x,0) =$	0, $i = 0, 2, 3, \ldots, m$, $j = 0, 1, \ldots, n$	$\delta_x(x,0) =$	$25 \cdot 10^{-6}$ m
$C_B(x,0) =$	7 kg QOD·m^{-3}	$\bar{S}_x(x,0) =$	$3.96 \cdot 10^{-2}$ m^2

Solutions have been approached by finite differences using the off-center explicit method and taking 50 nodes uniformly distributed along the reactor height.

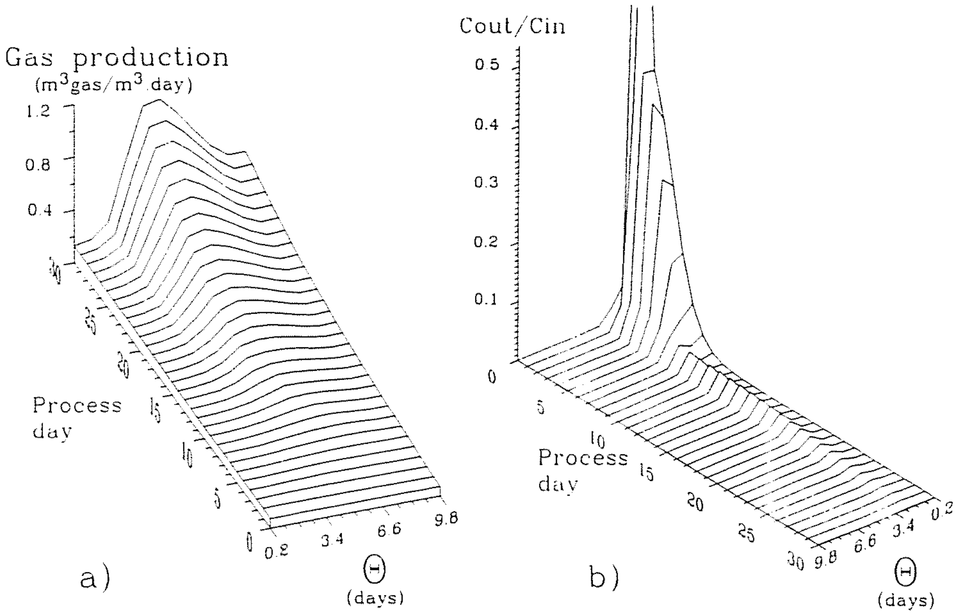

Fig. 1. Numerical simulation results for retention times between 0.2 and 9.8 days.
a) Evolution of gas production.
b) Evolution of the ratio between effluent aggregate concentration (Cout) and the overall aggregate fraction in the reactor (Cin)

Fig.1.a shows evolution of gas production and *Fig.1.b* shows the ratio between effluent aggregate concentration and the overall aggregate fraction concentration in the reactor. Numerical simulations show aggregates wash-out for retention times below 2.2 days that are consistent with experimental results. Reactor activity is due to biofilm exclusively at high loading rates (i.e. low retention times, at or below 2.2 days). Simulated biogas production presents a maximum near 4.8 days retention time as obtained in pilot plant data.

Aggregates reach the upper part of the reactor by flotation and particles with bubbles, poor in settling properties, are found in the effluent at high retention time, as was appreciated during experimental works.

Real averaged QOD depuration has been slightly greater than in numerical results above 5 days retention time. That may be due to the low biomass on substrate yield Y taken in the simulations.

4. Conclusions

A structured model based on the dynamics of a discrete bivariant distribution of particles, the biofilm dynamics and their interaction has been developed. Although multiple simplification assumptions and postulates are needed, it offers a methodological way to formulate hypotheses, to detect some limit situations and to achieve a mathematical synthesis of empirical knowledge about the considered phenomena. The results obtained by numerical simulation, applying boundary conditions for an upflow anaerobic filter reactor with oriented support, show the same pilot plant tendencies, validating the model qualitatively.

References

1. RITTMANN, B. E. – MCCARTY, P. L. (1980): Evaluation of Steady-state Biofilm Kinetics. *Biotechnology and Bioengineering*, Vol. 22, pp. 2359–2373.
2. TRULEAR, M. G. – CHARACKLIS, W. G. (1982): Dynamics of Biofilm Processes. *Journal WPCF*, Vol. 9, 54, pp. 1288–1301.
3. ATKINSON, B. – UR-RAHMAN, F. (1979): Effect of Diffusion Limitations and Flock-size Distribution on Fermentor Performance and Interpretation of Experimental Data. *Biotechnology and Bioengineering*, Vol. 21, pp. 221–251.
4. BEEFTINK, H. – SATUGAARD, P. (1986) Structure and Dynamics of Anaerobic Bacterial Aggregates in a Gas-lift Reactor. *Applied and Environ. Microbiology*, Vol. 52, pp. 1139–1146.
5. EDELSTEIN, L. – HADAR, Y. (1983) A Model for Pellet Size Distribution in Submerged Mycelial Cultures. *Journal Theor. Biol.*, Vol. 105, pp. 427–452.
6. BEEFTINK, H. – VAN DEN HEUVEL, J. C. (1990): Bacterial Aggregates of Various and Varying Size and Density: a Structured Model for Biomass Retention. *The Chemical Engineering Journal*, Vol. 44, pp. 1–13.
7. BRYERS, J. D. (1987): Biologically Active Surfaces: Processes Governing the Formation and Persistance of Biofilms. *Biotechnology Progress*, Vol. 3, 2, pp. 57–68.
8. FLOTATS, X. (1993): Liquid Fraction Pig Waste Treatment by an Anaerobic Filter with Oriented Support. Ph. D. Thesis, Universitat Politècnica de Catalunya, Barcelona, Spain.